Chapter 5:

Development of Chitosan Based siRNA Delivery System

5.1 Introduction

Recently, chitosan based non-viral vectors are used as a potential carrier for gene therapy, because of its excellent biocompatibility, safety, biodegradability in humans, and low immunogenic potential [1, 2]. Chitosan is positively charged at below the pKa (6.6) which can favour interaction with nucleic acids such as DNA or siRNA leading to formation of polyplexes with different size, shapes and properties.

The properties of chitosan are significantly influenced by solubility, pKa, molecular weight, degree of deacetylation [3]. The poor solubility of chitosan at physiologic pH translates into colloidally unstable polyplex. As the pKa of chitosan is about 6.6, it is unionized at physiologic pH, the neutral surface charge tend to aggregate due to the absence of an inter-particular repulsive force. The high molecular weight chitosan (100-400 kDa) forms extremely stable polyplex but have poor colloidal stability due to low solubility. They also tend to contribute to viscosity at concentrations suitable for gene delivery. The transfection efficiency is significantly influenced by working pH. As chitosan becomes positively in acidic conditions, the transfection efficiency is improved at lower pH 6.5-7.0, compared to 7.4 where chitosan is unionized [4, 5]

The low-charge density at physiological conditions is the primary reason for its low toxicity and may also facilitate intracellular release. However, this property also leads to premature dissociation of polyplex. The ideal polymer-based siRNA delivery systems satisfy the conflict requirements for the polymer-siRNA binding and provide a balance between protection and intracellular release [6]. Based on a recent study by atomic force microscopy, the inter-action strengths between siRNA and chitosan were pH dependent and the adhesive interactions decreased as the pH was increased from 4.1 to 6.1, 7.4, and 9.5 [7]. To overcome these limitations, various polymer modifications have been attempted to improve colloidal stability of chitosan such as PEGylation, to induce positive charge at physiologic pH through quarternization by the trimethylation of amino groups [8, 9].

Another important requisite for polymer based vector is high buffering capacity in endosomal pH range. Chitosan is reported to have buffer capacity even higher than that of PEI when compared at equal mass concentrations (chitosan at 4X mass of PEI). Most of the buffer capacity is derived from the free chitosan part of nucleic/acid complex. Further, the chitosan-DNA complex showed ~2 fold reduction in buffering capacity compared to free

chitosan, corroborating the role of free forms of chitosan [10]. However, this may require excessive amounts of polymer dosing. Further, the attempts to quaternize chitosan backbone may negatively affect the buffer capacity. Therefore, we devised an alternative strategy to overcome limitations of chitosan as a gene delivery vector.

5.2 Experimental

5.2.2 Overcoming physical instability of chitosan

5.2.2.1 Preparation of low molecular weight chitosan (LMWC)

Chitosan, medium molecular weight (MMWC) was purchased from Sigma Aldrich (Bangalore, India). Chitosan was depolymerized using nitrous acid due to the reproducible nature of procedure reported in literature [11]. In brief, 0.5% chitosan (w/v) was dissolved in 50 mM HCl overnight. Sodium nitrite ($NaNO_2$) was added at various levels in the range of 0.001–0.1 mole/mole of glucosamine and reaction was performed at room temperature for 24 hr. The reaction was stopped by precipitation using 2.5 N sodium hydroxide to bring the pH to 10. The precipitate was then washed by repeated centrifugation (10000 rpm for 15 min) and suspended in deionized water, until the supernatant reached neutral pH. The samples were freeze-dried prior to characterization and used in the production of nanoparticles. The concentration of $NaNO_2$ with respect to glucosamine was optimized to achieve desired viscosity-average molecular weight (Mv) of 30, 60, 90 kDa [12].

5.2.2.2 Characterization of LMWC

a) Molecular weight

Viscometric method for estimation of chitosan molecular weight are easy and rapid to perform and provide accurate results. Therefore, viscosity of chitosan in 0.2M HAc/ NaAc were measured using Ubbelohde capillary viscometer at 25 ± 0.1 ^{o}C in triplicate. The capillary diameter used was 0.63 mm. Solution concentration were adjusted based on sample viscosity so as to get a flow through time of 100-200 sec. Then six different concentrations were prepared for each and viscosity was first determined relative to that of water [13]. Then intrinsic viscosity was determined by the common intercept of both Huggins ($\eta sp/C \sim C$) and Kraemer ($\eta inh \sim C$) plots on the ordinate at $C = 0$.

b) Solubility

The improvement in solubility after depolymerisation was studied by turbidimetric method [13]. Briefly, LMWCs (2 mg/ml) were dissolved in 0.1% acetic acid solution, the pH of solution was adjusted with 1N NaOH and transmittance of the resulting solution was measured at 600 nm as a function of pH. The cloud point pH, i.e. the pH upto which transmittance was greater than 98%, and pH50 i.e. the pH at which transmittance is greater than 50% were monitored.

5.2.3 Overcoming siRNA binding of LMWC

5.2.3.1 Preparation of LMWC-Protamine conjugate

EDC (or EDAC; 1-ethyl-3-(3-dimethylaminopropyl) carbodiimide hydrochloride) is the most commonly used carbodiimide conjugation reagent for biological substances containing carboxylates and amines. EDC is water soluble, allowing for its direct addition without need of organic solvents. Both the reagent and isourea by-product are water soluble which can be easily removed by dialysis. The N-substituted carbodimide can react with carboxylic acids to form highly reactive, o-acylisourea intermediates. This active species then can react with a nucleophile such as a primary amine to form an amide bond [14].

The activation of C-terminal of protamine using EDC protocols has been accomplished in literature for different purposes such as polymer coating on to amine functionalized nanoparticles[15], Listeriolysin O for gene delivery[16], preparation of protamine dimers for efficient histone displacement [17]. Similarly chitosan has been coupled with many activated reagents for different purposes such as biomaterial applications [18, 19], surface functionalization [20, 21], drug loading and targeting [22, 23] etc.

Most literature for using EDC describe the optimal reaction medium to be at a pH from 4.7 to 6.0 [14]. However, when working with proteins and peptides, it has been reported that EDC-mediated amide bond formation effectively occurs between pH 4.5 and 7.5. Outside this pH range the conjugation reactions are claimed to proceed more slowly with lower yields. Sulfo-NHS esters are hydrophilic reactive groups that couple rapidly with amines on target molecules [24]. The non-sulfonated NHS esters are relatively water-insoluble and must be first dissolved in organic solvent before being added to aqueous

solutions. In contrast, sulfo-NHS esters are water-soluble, longer-lived, and relative more stable to hydrolysis in water.

The rationale conjugation was proposed based on preliminary experiments indicating:

1. Contribution to proton sponge in vector development: The LMWC samples were evaluated for proton sponge effect. The study showed that they have equivalent buffer capacity to that of branched PEI. Therefore, it was desired to retain this property of chitosan in the designed vector so that endosomal escape is achieved.
2. PS required for effective binding: The arginine rich protamine can effectively condense siRNA at low mass ratio. Therefore, gel retardation was used to verify the amount of PS required as siRNA binding partner in the conjugate. The gel retardation assay showed that protamine retarded siRNA at very low polymer/siRNA weight ratio.

The choice and amount of LMWC in the conjugate was dependent on improvement in proton sponge brought by the added amount of chitosan.

1. Chitosan has very good buffer capacity in endosomal pH range due to its pKa of 6.6-6.7.
2. The literature reports that chitosan weight has very good transfection efficiency [25].
3. The use of higher weight ratios of LMWC (20 kDa) has been reported to result in increased size with increase in weight ratios to > 400 nm at 20 and higher [26, 27].
4. Moreover, the total chitosan used at high N:P ratios has been reported to not completely participate in the formation of the nanoparticle, since the excess chitosan can be found in the filtrate when centrifugal concentration is performed [28]. The large excess of free chitosan has also been reported to interact with membrane components or interfere with cellular processes and thus reduces cell viability [26].
5. The higher amounts are speculated mainly to contribute to the improved stability [28]. However, such formulations are also reported to bring significant practical problems including limited dosing due to aggregation and the nonspecific effects of large quantities of soluble chitosan [29].

Protocol: The prepared LMWC were conjugated with PS at different ratios by covalent conjugation using carbodiimide chemistry, i.e. EDC/NHS crosslinking chemistry. Briefly,

100 mg of LMWC and PS at different concentrations was dissolved separately in 20 mM MES buffer. The pH was adjusted to 5.5 and 20 times molar excess of EDC was added to PS solution followed by sulfo-NHS. The activated PS solution was immediately added to LMWC solution. The conjugation reaction was carried out for 24h at room temperature. After completion of reaction, 0.1 N NaOH was added drop wise to increase pH of the media to 10. The precipitated conjugate was then centrifuged to remove the unreacted PS and reactants in the supernatant. The precipitate was washed three times and dried to get product.

5.2.4 Characterization of conjugate

5.2.4.1 Determination of conjugation efficiency

The determination of conjugation efficiency was based on estimation of amount of PS in the isolated reaction product. It was done through specific quantification of PS amount in conjugate on weight basis. There are various techniques to estimate proteins which can be used to measure the protein part in the conjugate which were evaluated one by one. However, since the PS is UV inactive, spectrometric methods were not useful. Therefore, derivatization/colorimetric methods were proposed, such as Bradfod assay (Coomassie Brilliant Blue G-250 dye), Bicinchonic acid etc. Both of these methods were handy in estimating PS from pure solutions; however, in presence of chitosan there was interference due to poor solubility of chitosan part in the basic conditions of the assay (pH=10).

Therefore, sample processing was changed to incorporate step for hydrolysis of the interfering chitosan part of the conjugate using $NaNO_2$ before performing the analysis. Briefly, the conjugate was dissolved in 0.05% HCL to which $NaNO_2$ was added and vortexed for 1 hr. Then the aliquot from the hydrolysed mix was subjected to PS estimation. However, both method showed poor reproducibility as the control sample, i.e. unconjugated chitosan, also showed colour development with these reagents, which could be due to the presence of N-acetyl amine bond, and non-specific nature of the assay. Therefore, a protein estimation method which is not based on peptide bond was desired.

Finally, the difficulty of analysing PS in presence of chitosan was solved by using another protein estimation method known as Sakaguche reaction. Though this method also requires basic reaction pH for final colour formation, the reaction is specific for arginine

residues which are present in PS and absent in hydrolysed chitosan residue. The hydrolysed chitosan sample (control) did not show any colour formation with the reagent; therefore, conjugate sample after pretreatment with $NaNO_2$ were successfully subjected for Sakaguche reaction to estimate PS content. The details of the protocol are given below:

The colorimetric quantification method was developed based on Sakaguche reaction for selective estimation of PS by UV spectrophotometer.

Reagents for sakaguche reaction-

- α-Naphthol: A 0.05% w/v solution, prepared by diluting with water a 0.5% solution in 95 % alcohol.
- Sodium hypobromite: A solution made by dissolving 2 gm. (0.64 mL) of bromine in 5% w/v cooled, sodium hydroxide solution to make a total volume of 100 mL.
- Urea: A 40% w/v solution of urea in water.
- Sodium hydroxide: A 10% w/v solution in water.

Procedure:

Briefly, 0.08 mg of $NaNO_2$ was added to depolymerize chitosan fraction of 10 mg conjugate in 50 mM HCl and vortex mixed for 1 h. A significant drop in viscosity was evident of completion of depolymerisation process. Before this, it was ensured that colour development assay is unaffected by added concentration of $NaNO_2$ by estimating PS in pure solution and from solutions containing $NaNO_2$. Then the prepared sample was taken in a tube and 5 ml water was added to it. The tube was cooled in an ice bath for 30 minutes. 1 mL of the sodium hydroxide solution was added followed by 1 mL of the α-naphthol solution. The tube was replaced in ice bath for 5 minutes, with occasional shaking. Then 0.1 mL of hypobromite solution was added followed by 1 mL of urea solution after 15 seconds. The tube was shaken vigorously between these two additions and immediately after addition of the urea. The tube was brought to room temperature and absorbance was measured at 528 nm. The calibration curve was prepared for PS content.

The method was validated for accuracy, precision and robustness. The accuracy of the method was studied on three quality control samples i.e. 20, 40 and 80 µg/ml were selected within the calibration range. Accuracy was assessed in terms of % bias and recovery. Repeatability was determined by analyzing different QC levels of analyte (n=9) as mentioned in accuracy. Inter and intra-day variations was studied to determine

intermediate precision of the proposed method. Inter–day variation study was carried out for 3 days (n=9). The % RSD of the predicted concentrations was taken as precision. The robustness of the method was tested for change in α-Naphthol concentration.

5.2.4.2 Preparation of Polyplex

The complexation efficiency of LMWC is function of charge density available for complexation, which can be influenced by pH of vehicle used for polyplex preparation. Therefore, all the polyplex were prepared in 5.5 pH sodium acetate buffer (20 mM). The stock solution of chitosan was also prepared in same solution. The required amount of polymer stock solution was added to vehicle. Then 100 pmole of siRNA was added to it and mixture was gently vortexed for 2 min, and incubated for 20, 40, 60 mins at room temperature. Various w/w ratios of polymer/siRNA were used to optimize the polyplexes.

5.2.4.3 Complexation Efficiency

1. Gel retardation assay

The binding of siRNA with chitosan was determined by agarose gel electrophoresis. A series of different polymer to siRNA weight ratios were prepared. A 1:6 dilution of loading dye was added to each well and electrophoresis was carried out at a constant voltage of 50 V in TBE buffer pH adjusted to 7.4 and containing 0.5 µg/ml ethidium bromide. The siRNA bands were then visualised under a UV transilluminator at 365 nm.

2. Centrifugation

The centrifugation was performed with the same procedure as in chapter 4, section 4.2.3.9.

5.2.4.4 Size and zeta potential

The polyplex prepared were subjected to size and zeta potential measurements. The hydrodynamic diameter of the polyplexes was determined by using dynamic light scattering using Zetasizer, Nano ZS series (Malvern Instruments, Germany). The prepared complexes were diluted appropriately with sodium acetate buffer pH 7.4 and measured at 25^{o}C. The zeta potential was measured by applying Smoluchowski's equation in the zeta sizer software. All the experiments were performed in triplicates.

5.2.4.5 Cytotoxicity of polymer conjugate

The cytotoxicity study was performed as per the same protocol mentioned in the section 4.2.5. The polymer concentration used were in the range of 25, 250, 500, 1000 ug/mL.

5.2.5 Stabilization of complexes

5.2.5.1 siRNA location

In order to stabilize the complex, preferential loading of siRNA on PS was desirable. Therefore, the polyplex preparation at optimized weight ratio for LMWC-29-PS-12 was modified. Briefly, polyplex were prepared in 7.4 pH sodium acetate buffer (20 mM) with batch volume of 15 µl and incubated for 20 min. After incubation the pH was adjusted to 5.5 by adding 5 µl of acetate buffer pH 4.0 (20 mM) and further incubated for 20 min.

An experiment was designed to prove the hypothesis that PS fraction serves as a carrier for siRNA delivery to overcome the weak binding affinity of LMWC. It was observed that the siRNA bound to LMWC can be released by depolymerization of the LMWC using $NaNO_2$. For this purpose, after incubation, the formed polyplex were exposed to $NaNO_2$ and incubated. The quantity of $NaNO_2$ (~8.0 µg $NaNO_2$/mg of LMWC) was chosen so as to suffice the depolymerization of LMWC quantity in optimized polyplex and release siRNA.

5.2.5.2 TPP crosslinking

It was essential to have higher stability for the complexes in the presence of extraneous environment such as serum and extracellular fluids. Therefore, the ionotropic gelation using tripolyphosphate (TPP) was used to harden the formed polyplexes. TPP, due to its anionic charge, electrostatically interacts with the cationic amino groups of chitosan, resulting in intra- and inter-molecular cross-linking [6]. For ionic cross-linking the glucosamine/TPP ratio is very important. The polyplex were prepared at the optimized weight ratio of polymer/siRNA. After 20min incubation, the pH of incubation medium was adjusted to 5.5 (using the modified protocol of section 5.5.2.1). This also ensures that chitosan will be sufficiently charged to undergo ionotropic gelation. TPP was added to the polyplex formulation at LMWC-29-PS-12 conjugate to TPP mass ratio of 9:1 and vortexed

and further incubated for 15 min. The polyplex were characterized for complexation efficiency, size and zeta potential.

5.2.6 Stability challenge studies

5.2.6.1 Heparin challenge study

The improvement in the relative stability of LMWC-29, LMWC-29-PS-12 and TPP cross-linked LMWC-29-PS-12 polyplexes was checked using resistance to heparin challenge assay. The heparin challenge study was performed according to same protocol as mentioned section 4.2.6.2.

5.2.6.2 Serum Stability

The naked siRNA, LMWC-29-PS-12 and TPP cross-linked LMWC-29-PS-12 polyplexes were subjected to serum stability study according to same protocol as mentioned in 4.2.6.3.

5.2.6.3 Stability in brochoalveolar lavage fluid

The same protocol as mentioned in section 4.2.6.4 was used to study the stability of LMWC-29-PS-12 and TPP cross-linked LMWC-29-PS-12 polyplexes in brochoalveolar lavage fluid.

5.2.7 Transmission electron microscopy

Transmission electron microscopy (TEM) was performed to study the morphology of particles using Cryo-TEM (TECNAI G2 Spirit Bio TWIN, FEI-Netherlands) operating at 200 kV with resolution of 0.27 nm. Briefly, glow discharge was used to convert the hydrophobic grid into hydrophilic. The formulation was spread on the grid and cryo-freezed in liquid nitrogen ethane at -180^{o}C. Using a cryo-holder the grid was inserted into microscope and images were taken.

5.2.8 Proton sponge

For successful transfection it was essential that the formulation undergoes endosomal escape. The property is directly proportional to the buffer capacity of the carrier in the endosomal pH range i.e. 5.5 to 7.4. Therefore, proton sponge study was carried out. In case of chitosan, as it was insoluble at alkaline pH and took time to dissolve during titration, the study was done by titrating polymer solution from solution in acidic to basic pH [10].

Briefly, 10 mg of the polymer was dissolved in 150 mM NaCl solution with help of HCl and initial pH was adjusted to 3.5 and then titrated with 0.1 N NaOH solutions. The pH values were recorded with a pH Meter (Lab India,). The electrode was calibrated with buffer solutions of pH 4, 7 and 9.2. The amount of titrant consumed was calculated and compared.

5.3 Result and Discussion

5.3.1 Preparation and characterization of LMWC

The increased solubility of depolymerized chitosan could prove advantageous to overcome the colloidal stability of chitosan, therefore LMWC were prepared to achieve the same. There are different methods for depolymerisation of chitosan such as oxidative degradation, enzymatic, acidic cleavage and ultrasound degradation. The $NaNO_2$ based oxidative degradation was used for depolymerization due to its good reproducibility as compared to other methods utilizing enzymatic, acidic cleavage and ultrasound degradation [11, 13, 30]. The depolymerization occurs through deamination of (1 → 4)-linked 2-acetamido-2-deoxy-β-D-glucopyranose unit resulting in formation of 2, 5-anhydro-D-mannose at the new reducing end. Desired molecular weights were obtained by changing chitosan/$NaNO_2$ molar ratio while maintaining constant reaction temperature and time. The linearity between chitosan/$NaNO_2$ molar ratio and obtained molecular weight was used to fine tune the target molecular weight.

The viscosity average molecular weights (Mv) for the depolymerized chitosan sample were determined by using Mark–Houwink's equation [19]. The specific viscosity (ηsp) was determined for different concentrations(C) of sample from which the reduced viscosity (ηsp/C) and inherent viscosity was calculated. Straight-line fits were observed for all chitosan fragments (R^2 >0.95). The intrinsic viscosity [η] was obtained by extrapolating the common intercept of both Huggins (ηsp/C ~ C) and Kraemer (ηinh ~ C) plots on the ordinate at C=0 [20], as shown in Fig. 5.**1**. Finally, the viscosity average molecular weight (Mv) using the relation:

$$[\eta] = K (M_v)^{\alpha}$$

Where, [η] is the intrinsic viscosity, K and α are the constants obtained from literature, as a measure of solute-solvent interaction ($K = 1.38 \times 10^{-5}$ and $\alpha = 0.85$) [14, 21, 22]. Finally,

the LMWCs of 29, 53, 88 kDa (henceforth labelled as: LMWC-29, LMWC-53, LMWC-88 respectively) were selected for further screening for favourable vector development properties to be suitable for delivery of siRNA.

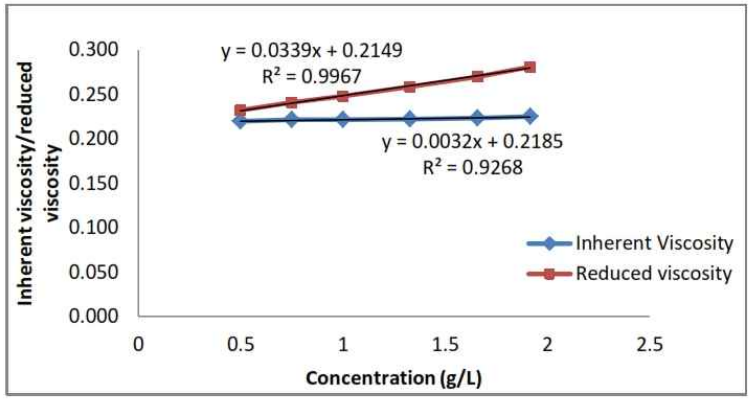

Fig. 5.1: Representative plot for intrinsic viscosity calculation (LMWC-88)

The depolymerized chitosan showed a significant reduction in intrinsic viscosity compared to large molecular weight chitosan (Table 5.1). The LMWC-29 had 9 fold reduced viscosity than high molecular weight chitosan. This is good indicator for resulting into a more preferable size range. It has been reported that lower intrinsic viscosity is indicator of condensed state and promotes formation of compact structures during polyplex formation or ionic cross-linking leading to a decreased particle size [36, 37].

Table 5.1: The calculated intrinsic viscosity of Chitosan and LMWC fragments

Name	Molecular weight (Mv)	Intrinsic Viscosity (dl /g)
LMWC-29	28900 Da	0.85435
LMWC-53	52758 Da	1.425029
LMWC-88	87920 Da	2.199649

The LMWCs were characterized for solubility profile using turbidimetry to study the effect of depolymerisation on colloidal stability of LMWCs. With change in molecular weight the pH dependent solubility was altered which was detected by change in transmittance. A correlation was found for transmittance and pH for all chitosan. The transmittance was found to decrease with increase in pH for all LMWCs from which pH50 and cloud point was determined (Fig. 5.2). As expected the pH_{50} and cloud point increased

with decrease in molecular weight due to increase in solubility. Chitosan solubility is a function of degree of polymerization, which allowed use of molecular weight reduction to increase the solubility. The effect can be attributed to the reduced inter-chain interactions between short chains of LMWCs [13, 38].

However, the objective was to obtain LMWCs with good colloidal stability around physiologic pH. The soluble-insoluble transitions are initiated at pH around the pKa of amino groups of chitosan (i.e. 6.5 – 6.8). From the transmittance values, it was apparent that LMWC-29 was having good solubility near physiologic pH. The cloud point was 7.2 while the pH_{50} was well above 8.0. For LMWC-53 and LMWC-88 precipitation occurs at pH values below 7.0 and more than 50% transmittance was reduced at 7.6 and 7.1, respectively. Therefore, only LMWC-29 was found appropriate for desired vector development due to superior solubility and colloidal stability and thus chosen for further experiments. The LMWCs tend to bring optimal physicochemical properties to formulation through effects on size and zeta potential [4].

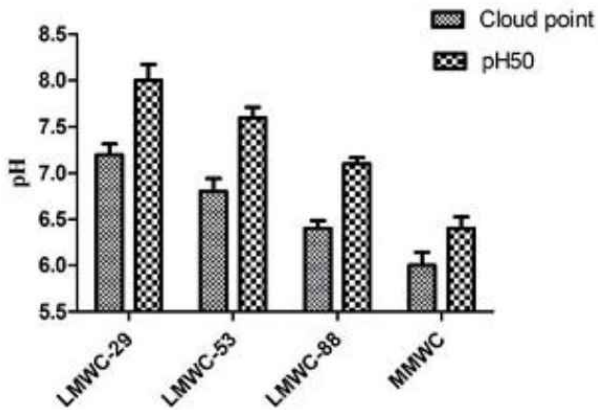

Fig. 5.2: Solubility profile of different molecular weight chitosan

5.3.2 Preparation and characterization of LMWC-PS conjugate

The delivery of nucleic acids is challenged by milieu of extracellular and intracellular challenges, wherein the binding between vector and siRNA cargo play a vital role in deciding success of delivery. Specifically, the weak polymer-siRNA binding affinity has been correlated to poor cell uptake and transfection due to premature release of siRNA which cannot cross the cell membrane and are degraded by the endogenous nucleases [39,

40]. In contrast, after reaching the intracellular site, polyplexes may fail due to inefficient unpacking of siRNA due to tight polymer-siRNA binding [41]. Thus, an ideal polymer-based siRNA delivery systems should be designed by giving consideration to the requirement of polymer-siRNA binding accounting for a subtle balance between desired protection and intracellular release of siRNA [6].

Depolymerization of chitosan have been found to improve the solubility and dose-dependent cytotoxicity [42]. However, this step leads to diminished stability of polyplex. Particularly, the binding affinity has been stated as rate limiting in determining polyplex transfection efficiency [4, 43]. They have been cited to improve the release of nucleic acids from weak complexes formed with depolymerized chitosans leading to improved transfection compared to that achieved with high molecular weight chitosan [13]. At the same time, the incapability of depolymerized chitosans to protect DNA from degradation by DNases and serum components as well as poor uptake of polyplex has also been reported [23]. Hoggard et al. reported that chitosan oligomers form weak polyplexes which dissociate in presence of salt and result in low gene transfection [44]. The biophysical aspects of chitosan/siRNA have been studied to correlate polymer/siRNA interaction with bioactivity [36]. The literature values of dissociation constant (Kd) obtained through isothermal titration calorimetry (ITC) suggests that Kd values of less than 1 for chitosan with MW 44 kDa. However, it sharply increases to 1.5 and 1.9 for MW of 63 and 93 kDa, respectively [36].

Some studies have stated that to overcome these limitation excess of chitosan with N:P of 150 is required [45]. However, such approach will need excessive amount of vector dose, therefore; other strategies are desired. Chitosan has very good buffer capacity in the endosomal pH range due to presence of amino groups. The strategies based on modification of amino functional group, such as preparation of trimethyl chitosan, may lead to loss of proton sponge capacity. Therefore, approach was desired to provide the sufficient protection to bound siRNA to chitosan and help in escaping the complexes from endosomal compartment and to enhance the cytoplasmic release of nucleic acids by incorporating proton sponge.

The protamine antibody fusion protein has been used to target siRNA to HIV-infected or envelope-transfected cells, wherein the PS serves as binding partner for

negatively charged siRNA whereas heavy chain antigen binding region helps in specific receptor interaction [46-48]. Similarly, liposomes-protamine-HA nanoparticle as well as siRNA/DNA protamine nanoparticle have been reported for taking advantage of nucleic acid binding property of protamine sulphate [49-52]. Therefore, here we combined the nucleic acid binding property of PS with buffer capacity of colloidally stable LMWC. This was achieved through preparation of conjugates through EDC-NHS carbodimide chemistry as discussed above.

In order to characterize the conjugate for conjugation efficiency, analytical method was developed to determine the content of PS in conjugate on weight basis. The method was based on principle that PS can be detected using the Sakaguche reaction, however, the interference of chitosan during the reaction can be removed by depolymerizing it at the beginning of the sample preparation. Fig. 5.3 shows the overlay of calibration curve for 10, 20, 30, 40, 60, 80, 100 µg/mL concentrations of PS. The linearity range was found to be 10 – 100 µg/mL. The linear regression equation obtained was Absorbance = [0.0079 x conc. in µg/ml] - 0.0866; with regression coefficient of 0.99 (Fig. 5.4).

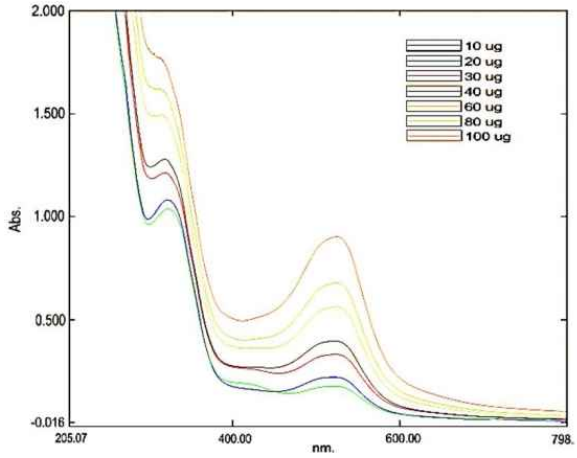

Fig. 5.3: Spectral overlay of different calibration standards

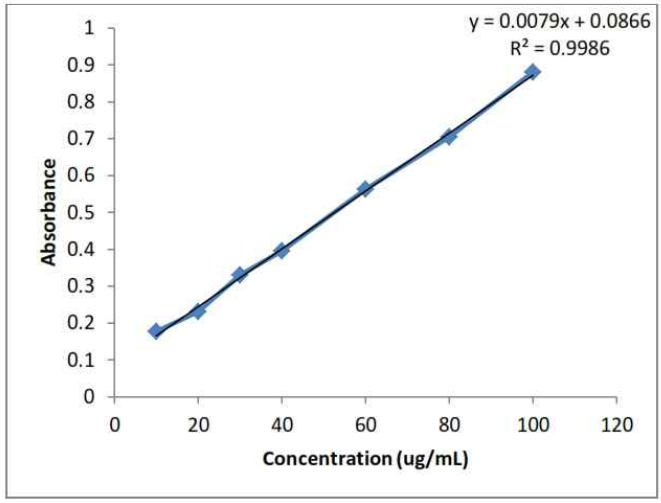

Fig. 5.4: calibration of colorimetric method for estimation of PS

Fig. 5.5 shows overlaid spectra of PS in presence of chitosan confirm the absence of interference at the wavelength used (528 nm). This indicates the selectivity and specificity of the proposed method. All three QC levels (LQC, MQC and HQC) showed an accuracy (% bias) ranging from 1.87 to 3.0%. The mean % recovery values and their low SD values represent the accuracy of the method (Table 5.2). In repeatability study, the % RSD ranged from 1.03 to 2.74 %. RSD values were significantly low for intermediate precision, with intra-day variation not more than 2.2 % and inter-day variation not more than 2.74%

(Values are represented as mean ± SD, n = 3

Table 5.3). Lower % RSD values indicated the repeatability and intermediate precision of the method. The Sakaguche reaction is sensitive to change in concentration of α-Naphthol solution, the robustness of method for chosen concentration of α-Naphthol was tested. The method was subjected to 5% change in concentration of α-Naphthol was evaluated and it was observed that method had acceptable level of recovery between 97.69 to 103.49 %.

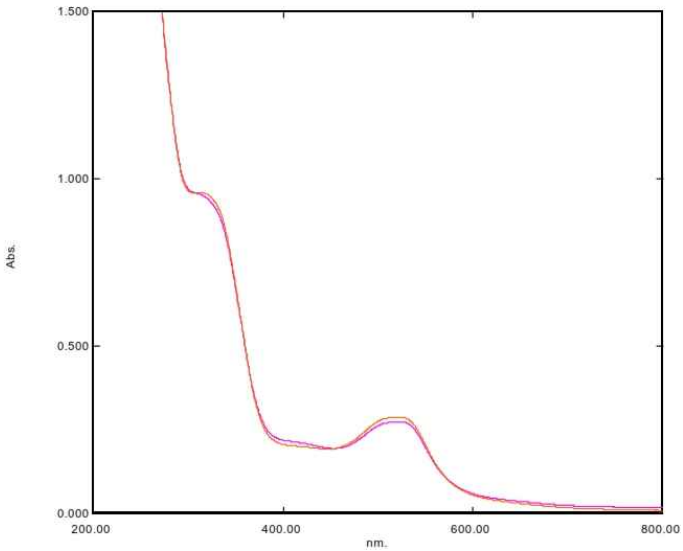

Fig. 5.5: The overlay of spectra of PS and chitosan showing absence of interference

Table 5.2: Results of Accuracy measurements

Level	Expected conc. (µg/ml)	Observed conc. (µg/ml) ± S.D	Mean % Recovery	% Bias
LQC	20	20.6 ± 0.190	103	3.0
MQC	40	40.8 ± 0.169	102	2.0
HQC	80	81.5 ± 0.282	101.87	1.87

Values are represented as mean ± SD, n = 3

Table 5.3: Inter and Intra-day Precision

Conc.(µg/ml)	Observed Conc.(µg/ml) ±SD		% RSD	
	Intraday Precision	Interday Precision	Intraday Precision	Interday Precision
20	20.9 ± 0.459	20.44 ± 0.560	2.20	2.74
40	38.8 ± 0.533	40.52 ± 0.489	1.37	1.21
80	81.2 ± 0.908	81.78 ± 0.846	1.12	1.03

Values are represented as mean ± SD, n = 3

Table 5.4: Robustness of method for change in α-Naphthol addition

Conc.(µg/ml)	Mean % Recovery ±SD	
	-5% α-Naphthol	+5% α-Naphthol
20	98.92 ± 0.423	102.79 ± 0.509
40	98.06 ± 0.394	101.51 ± 0.434
80	97.69 ± 0.373	101.48 ± 0.563

Values are represented as mean ± SD, n = 3

After trial and optimization of reaction conditions the following conjugate products were obtained (Table 5.5). The method for product isolation from the excess of reactant mixture, after completion of reaction, was validated by performing isolation of physical mixture by same method wherein the precipitate obtained after centrifugation were analysed by the above method and were found to contain no PS (data not shown). Finally, the products obtained after actual reaction were tested using the developed method and conjugation efficiency was determined. The obtained conjugation efficiency were verified within the analytical verification. The obtained conjugation efficiency were labelled for the purpose of convenience to the nearest digit.

Table 5.5: Conjugation efficiency of the conjugates

Sr No	Conjugation Efficiency (%)	Nomenclature used
1.	5.2±1.54	LMWC-29-PS-05
2.	11.8±1.79	LMWC-29-PS-12
3.	17.1±2.13	LMWC-29-PS-17

Values are represented as mean ± SD, n = 3

5.3.2.1 Complexation efficiency

The gel electrophoresis of MMWC showed retardation at weight ratio of 4 and more. On the other hand the LMWC-29 was able to condense the siRNA at weight ratios of 28 (Fig. 5.6 and Fig. 5.7). Thus, the MMWC is able to condense siRNA at relatively lower weight ratios. This was due to the large molecular weight which effectively condenses the siRNA. Literature has reported that high molecular weight chitosan have higher binding constants compared to LMWCs. The literature values of dissociation constant (Kd) obtained through isothermal titration calorimetry are less than 1 for chitosan with MW 44 kDa. However, it

sharply increases to 1.5 and 1.9 for MW of 63 and 93 kDa respectively [36]. This results in requirement of higher weight ratios of LMWC-29 for complete retardation of siRNA on gel electrophoresis.

In contrast, the cationic peptides, PS showed very good binding affinity due to high charge density. Fig. 5.8 shows gel retardation assay of PS. It was able to retard siRNA at PS/siRNA weight ratio of 1.5. It has been reported in literature that apart from high charge density of PS, the distance between the charged guanidine residues plays a critical role in imparting strong binding.

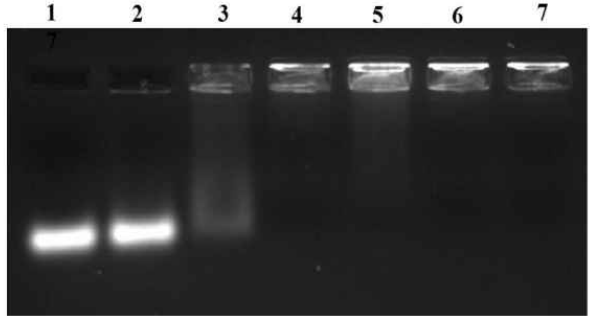

Fig. 5.6: Gel retardation assay of MMWC

(Polymer/siRNA w/w ratio) → Lane 1: Naked siRNA, Lane 2: 2, Lane 3: 3, **Lane 4: 4**, Lane 5:5, Lane 6: 6, Lane 7: 7

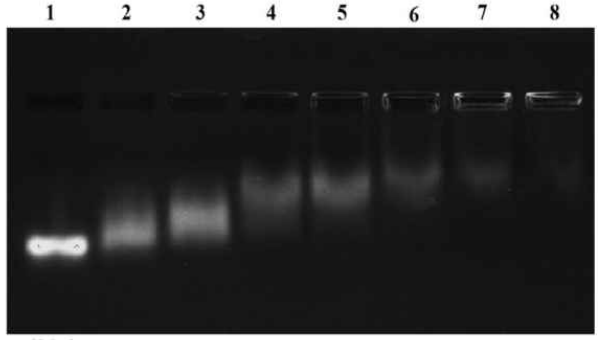

Fig. 5.7: Gel retardation assay of LMWC-29

(Polymer/siRNA w/w ratio) → Lane 1: Naked siRNA, Lane 2: 4, Lane 3: 8, Lane 4: 12, Lane 5: 16, Lane 6: 20, Lane 7: 24, **Lane 8: 28**

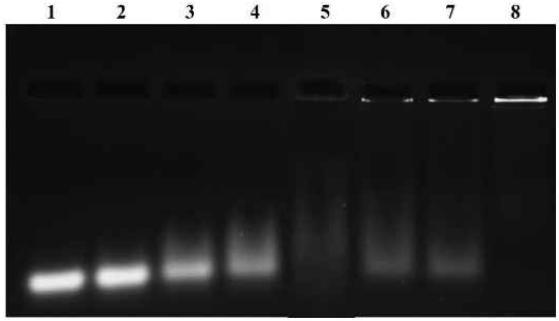

Fig. 5.8: Gel retardation assay of PS

(Polymer/siRNA w/w ratio) → Lane 1: Naked siRNA, Lane 2: 0.1, Lane 3:0.25, Lane 4:0.5, Lane 5:0.75, Lane 6: 1.0, Lane 7:1.25, **Lane 8: 1.5**

The conjugates were obtained with different degree of conjugation from 5, 12 and 17% PS on weight basis. The LMWC-29-PS-05 was unable to retard the siRNA and required 24 weight ratio for complete retardation. While LMWC-29-PS-12 and LMWC-29-PS-17 were able to retard siRNA at 16 and 10 weight ratio respectively. Fig. 5.9, shows the gel retardation assay of LMWC-29-PS-12 conjugate. Thus, from gel retardation it was concluded that conjugation of PS with LMWC was able to overcome the low complexation capacity of LMWC.

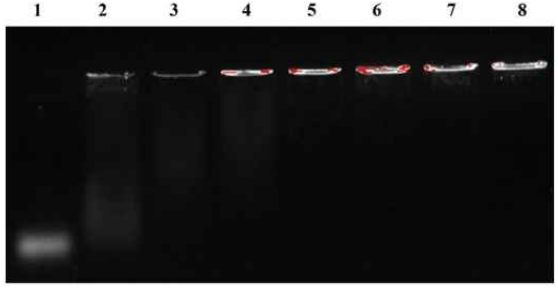

Fig. 5.9: Gel retardation assay of LMWC-29-PS-12 conjugate

(Polymer/siRNA w/w ratio) → Lane 1: naked siRNA, Lane 2: 4, Lane 3:8, Lane 4:12, **Lane 5:16,** Lane 6: 18, Lane 7:20, Lane 8: 24

To quantitate the complexation efficiency at the weight ratio resulting in complete retardation in gel electrophoresis centrifugation-UV spectrophotometric analysis was performed. siRNA polyplex were centrifuged at 25,000 rpm for 45 min at 4°C. The aqueous supernatant from these centrifuged sample was separated and analyzed for siRNA

content using NanoDrop UV spectrophotometer. Table 5.6 shows the complexation efficiencies of complexes.

Table 5.6: Complexation efficiency at the optimized weight ratios

Formulation	w/w ratio	Complexation Efficiency (%)
MMWC	4	96.58±1.72
LMWC-29	28	93.27±2.16
PS	1.5	98.18±1.54
LMWC-29-PS-05	24	95.36±1.76
LMWC-29-PS-12	16	97.88±1.35
LMWC-29-PS-17	10	97.58±1.19

Values are represented as mean ± SD, n = 3

5.3.2.2 Size and zeta potential

The size and zeta potential was measured at pH 7.4 the results are depicted in Table 5.7. The MMWC formed very large **size** polyplex due to long linear chains. In contrast, LMWC-29 forms much smaller polyplexes. PS due to its smaller peptide length and formation of tightly condensed polyplexes due to higher charge density forms very small polyplexes. The conjugates show properties midway of LMWCs and PS. The PDI values were acceptable for all the formulations.

As the chitosan is unionized at pH 7.4, the MMWC and LMWC showed very low values of zeta potential (Table 5.7). In case of PS the zeta potential values were high, as the pKa value of arginine groups is ~12, which results in generation of a cationic charge over PS at pH 7.4. The LMWC-PS conjugates also showed similar trend of higher zeta potential as they contain positively charged PS. The magnitude of zeta potential indicates charge density, it was very insignificantly affected by the changes in PS content in conjugates, since they would retain same charge density.

Table 5.7: Size determined at optimized polymer to siRNA weight ratios

Formulation	Particle Size (nm)	PDI	Zeta Potential (mV)
MMWC	446.3±8.8	0.322±0.025	+2.86±0.85
LMWC-29	295.5±6.4	0.286±0.021	+4.13±0.79
PS	158.2±3.7	0.140±0.012	+16.59±1.26
LMWC-29-PS-05	305.4±5.4	0.285±0.018	+7.64±0.65
LMWC-29-PS-12	292.1±3.9	0.253±0.017	+14.33±1.18
LMWC-29-PS-16	283.0±4.2	0.211±0.019	+15.28±1.24

Values are represented as mean ± SD, n = 3

5.3.2.3 Cytotoxicity study

Fig. 5.10 shows the viability of CFBE 41o- cells after 24h incubation with different concentrations of the polymer. The concentration ranged from 25, 250, 500, 1000 ug/mL. All the chitosan based polymer and conjugate showed negligible toxicity i.e. > 90% after 24h at concentration of 25, 250, 500, 1000 ug/mL in CFBE cells. In case of PS the cell viability at concentrations greater than 250 ug/mL and was ~70% after 24h at 1000 ug/mL. Which means that PS as such is toxic to the cells, however; when used in the form of conjugate the toxicity is significantly reduced. This was expected as PS was only a small fraction of conjugate and is associated with chitosan, which can alter physiologic effects displayed by free PS.

Based on studies of gel retardation, complexation efficiency, size and zeta potential and biocompatibility studies it was observed that conjugate displayed better physicochemical properties compared to both MMWC, LMWC-29 and PS alone. 5% conjugation was requiring higher weight ratios for complete retardation and also showed less complexation efficiency. The 12 and 17% conjugation showed equal effect in gel retardation, size and zeta potential. There wasn't significant benefit of increasing PS from 12 to 17% in both complexation and size and zeta potential. Further, the PS alone was found to be toxic at higher concentrations, therefore, it was not considered prudent to go with higher concentrations of PS and 12% conjugation was concluded to be optimum for carrier properties.

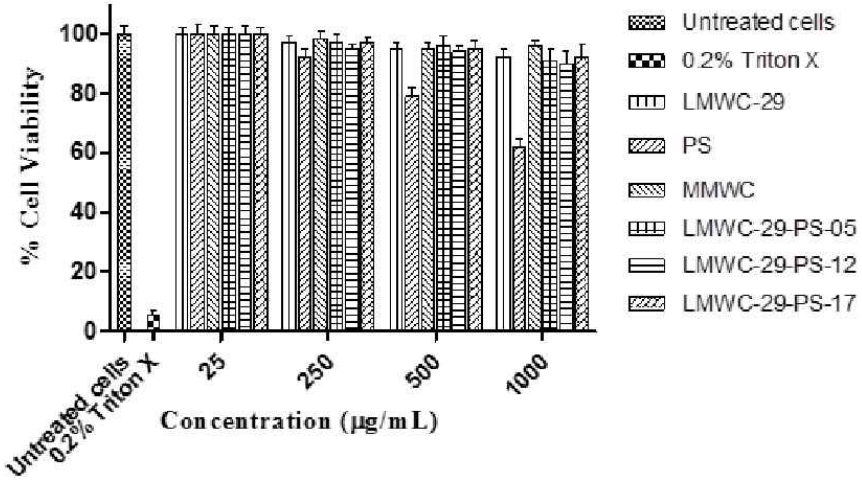

Fig. 5.10: MTT assay for cytotoxicity of chitosan polymers

5.3.3 Stabilization of polyplex

5.3.3.1 siRNA location

The higher charge density of PS than chitosan and its ionized state relative to chitosan which is unionized at 7.4 pH can be used to induce binding of siRNA preferentially PS fraction, and leaving negligible portion on the chitosan. This can also overcome the pH dependent binding affinity of LMWC, which have weak affinity to siRNA at 7.4 pH. This is also responsible for premature release of nucleic acids from chitosan based vectors at physiologic pH conditions. Therefore, during polyplex preparation, siRNA addition and incubation with polymer solution was performed at 7.4 pH where only PS is ionized and then pH was reduced to 5.5.

It was observed that the siRNA bound to LMWC can be released by depolymerization of the LMWC using $NaNO_2$. Therefore, after preparation, all polyplex were treated with $NaNO_2$ and incubated. Fig. 5.11 shows that, $NaNO_2$ does not affect the integrity of siRNA (lane 2) and shows same intensity as that of naked siRNA in presence of $NaNO_2$. The lane 3 shows that $NaNO_2$ treatment does not liberate siRNA, if bound to pure PS. While the lane 4, shows that $NaNO_2$ can release siRNA bound to LMWC. Finally, the lane 5 & 6 shows that $NaNO_2$ treatment could not release the siRNA from the LMWC-29-

PS-12 conjugate (duplicate runs), indicating that siRNA is bound to PS fraction of conjugate. However, heparin can release siRNA bound to PS as well. Therefore, the presence of siRNA in retarded wells was confirmed by addition of heparin to all the wells when the run was 50% complete. Fig. 5.12 shows that lane 3 release siRNA bound to PS. Similarly, lane 5 & 6 released siRNA bound to PS fraction of conjugate.

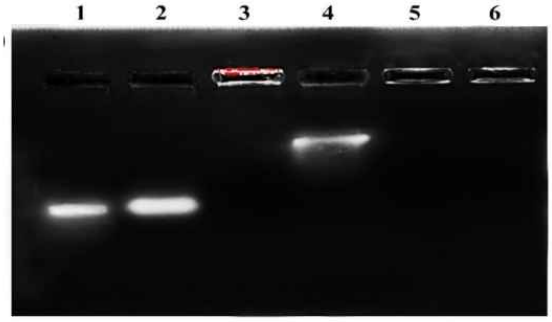

Fig. 5.11: Gel retardation showing location of siRNA

Lane 1: naked siRNA, Lane 2: siRNA + $NaNO_2$, Lane 3: siRNA+PS+$NaNO_2$, lane 4: siRNA+LMWC-29+$NaNO_2$, Lane 5 & 6: LMWC-29-PS-12 + $NaNO_2$

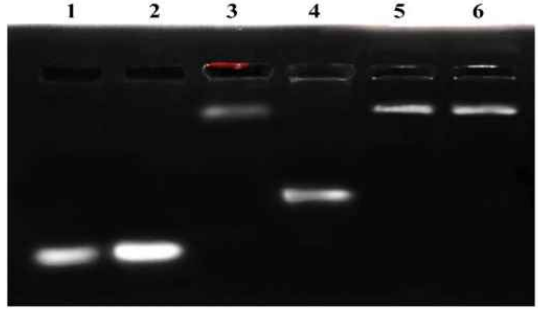

Fig. 5.12: Confirmation of siRNA in retarded wells after displacing with heparin

Lane 1: naked siRNA, Lane 2: siRNA + $NaNO_2$, Lane 3: siRNA+PS+$NaNO_2$, lane 4: siRNA+LMWC+$NaNO_2$, Lane 5 & 6: LMWC-29-PS-12 + $NaNO_2$

5.3.3.2 TPP cross-linking

The optimized weight ratio of LMWC-29-PS-12 conjugate to siRNA was subjected to ionic cross-linking with TPP to make polyplex rigid and improve the stability. In the present studies, based on preliminary trials, LMWC-29-PS-12 conjugate to TPP mass ratio of 9:1

was used to ionic cross-link, since at lower ratios result in formation of larger aggregates [53]. Before actual experiment, it was also confirmed that higher concentration of anionic TPP do not negatively affects the binding affinity of siRNA to cationic polymer. In presence of TPP also, the complete retardation was observed at optimized weight ratio (data not shown). Further, it did not affect the integrity of siRNA.

Table 5.8 shows the results for entrapment efficiency, size and zeta after TPP cross-linking. The complexation efficiency was insignificantly affected compared to that of without TPP. However, the size and PDI showed improvement. The size and PDI both were reduced. It was attributed to the cross-linking ability of TPP, which would have led to condensation and homogeneity in the polyplexes. The zeta potential was found to be slightly decreased. Almalik et al. have reported that chitosan with molecular weight of 10 and 25 kDa form nanoparticles with size in the range of 100-200 nm. On the other hand Chitosan with higher molecular weight, 70 kDa and 684 kDa, form higher sized nanoparticles due to their less effective complexing ability [55, 56].

Table 5.8: Effect of TPP cross-linking on physicochemical parameter

Parameter	Value
Complexation efficiency (%)	97.67±1.55
Size (nm)	143.7±4.56
PDI	0.189±0.011
Zeta potential (mV)	+12.8±1.38

5.3.4 Stability challenge studies

5.3.4.1 Heparin challenge study

Although LMWC-29-PS-12 polyplexes showed complete retardation with good complexation efficiency, the affinity can be overcome by competition from polyanions present *in vivo* or extracellular matrix. Heparin is good simulator to study these properties of formulations. The resistance to heparin competition assay depends on binding affinity of siRNA with the carrier. Stability up to heparin/siRNA weight ratio of >1 is appropriate for achieving adequate *in vivo* stability [57].

The LMWC-29 formulation showed displacement from w/w ratio of 0.5 (Fig. 5.13). Finally, 100% dissociated at heparin/siRNA weight ratio of 1.5-2. Thus, LMWC-29 had

low resistance to polyanion competition which can be attributed to lower affinity of LMWC to the siRNA. The LMWC-29-PS-12 also showed lower resistance to polyanion competition as it started to displace siRNA from weight ratio of 1, while complete release occurred at weight ratio of 2. However, stabilized TPP cross-linked LMWC-29-PS-12 polyplex showed increase in resistance, as it started to release siRNA from weight ratio of 1.5, while complete displacement occurred at weight of 2-3.

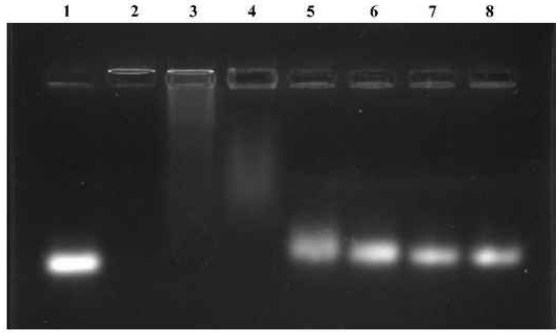

Fig. 5.13: Heparin resistance of LMWC-29 polyplex

Heparin/siRNA w/w ratio → Lane 1: naked siRNA, Lane 2: 0.25, Lane 3: 0.5, lane 4: 1.0, Lane 5: 1.5, Lane 6: 2.0, Lane 7: 3.0, Lane 8: 4.0

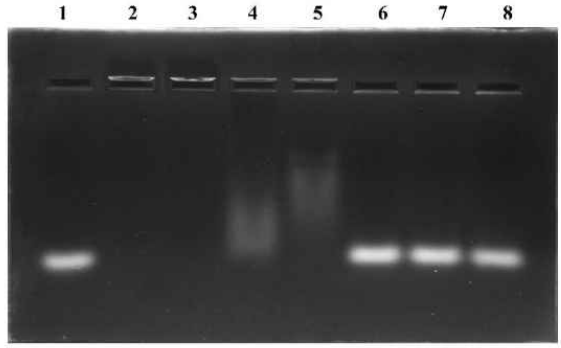

Fig. 5.14: Heparin resistance of LMWC-29-PS-12 polyplex

Heparin/siRNA w/w ratio → Lane 1: naked siRNA, Lane 2: 0.25, Lane 3: 0.5, lane 4: 1.0, Lane 5: 1.5, Lane 6: 2.0, Lane 7: 3.0, Lane 8: 4.0

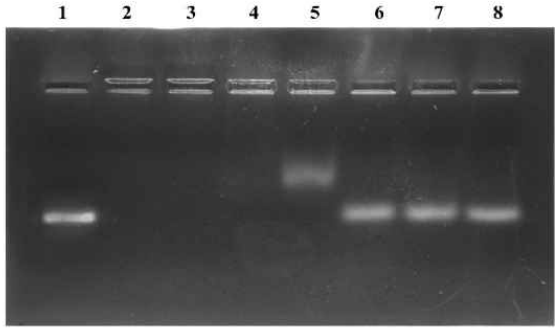

Fig. 5.15: Heparin resistance after TPP cross-linked LMWC-29-PS-12 polyplex Heparin/siRNA w/w ratio → Lane 1: naked siRNA, Lane 2: 0.25, Lane 3: 0.5, lane 4: 1.0, Lane 5: 1.5, Lane 6: 2.0, Lane 7: 3.0, Lane 8: 4.0

5.3.4.2 Serum Stability Study

To further confirm the ability of the formulations to survive in *in vivo* conditions, the serum stability study was conducted. Fig. 5.16, shows gel electrophoresis analysis of TPP cross-linked LMWC-29-PS-12 polyplex during serum stability. The formulations were able to retain more than 80% of siRNA up to 24h specifically the TPP cross-linked LMWC-29-PS-12 polyplex had > 90% retained siRNA**.** The LMWC-29-PS-12 polyplex retained about 77% of the siRNA after 24 h. The naked siRNA was degraded in 6h. This shows that TPP cross linking resulted in greater nuclease protection of siRNA in the serum than the LMWC-29-PS-12 and the protection was very significant compared to naked siRNA. Thus, as observed in the heparin resistance study the TPP cross-linking led to improved serum stability.

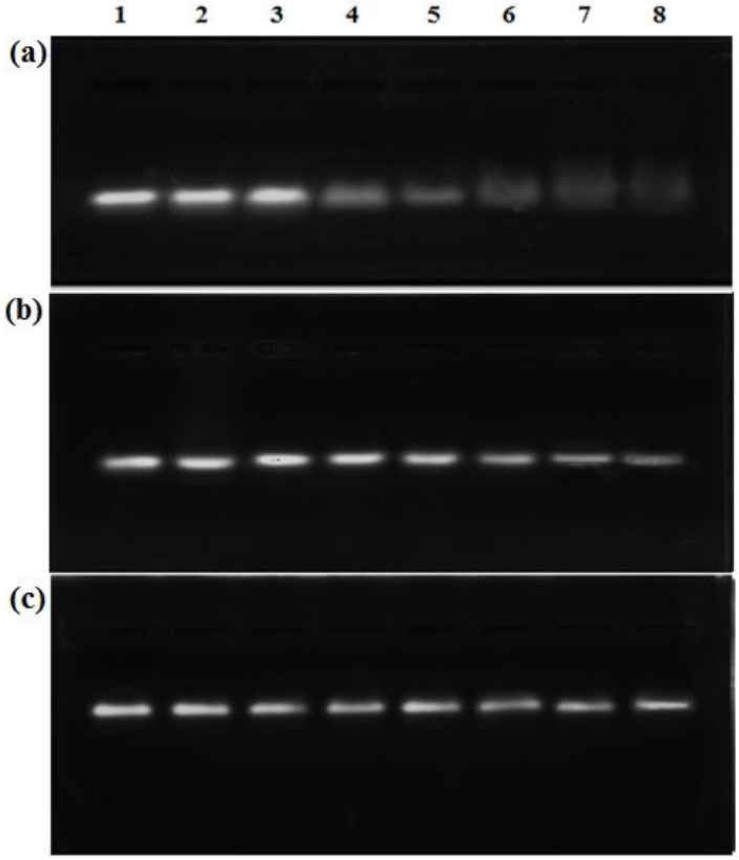

Fig. 5.16: Gel electrophoresis of serum stability

(a) Naked siRNA; 1=0h, 2=0.5h, 3=1.0h, 4=2.0h, 5=3.0h, 6=4.0h, 7=5.0h, 8=6.0h

(b) LMWC-29-PS-12; 1=0h, 2=1.0h, 3=2.0h, 4=4.0h, 5=8.0h, 6=16h, 7=20h, 8=24h

(c) TPP cross-linked LMWC-29-PS-12; 1=0h, 2=1.0h, 3=2.0h, 4=4.0h, 5=8.0h, 6=16h, 7=20h, 8=24h

Table 5.9: % siRNA retained during the course of serum stability study

Time (hr)	% siRNA retained	Time (hr)	% siRNA retained	
	Naked siRNA		LMWC-29-PS-12	TPP cross linked LMWC-29-PS-12
0	100.00	0	100.00	100.00
0.5	86.38±1.89	1	97.75±1.37	98.71±1.59
1.0	72.44±2.31	2	94.27±2.65	97.39±1.41
2.0	42.39±2.46	4	92.22±2.32	93.46±2.18
3.0	29.58±3.78	8	88.45±4.02	93.59±2.86
4.0	18.58±3.54	16	81.24±3.55	94.22±3.63
5.0	11.72±4.85	20	79.68±3.26	89.29±3.52
6.0	6.09±4.21	24	77.33±4.78	90.14±4.29

5.3.4.3 Stability in brochoalveolar lavage fluid

siRNA released from formulation after incubation form different time periods with BALF was determined using densitometry. The results are shown in Table 5.10. It was observed that with increase in incubation time siRNA retained was decreasing (Fig. 5.17). This was attributed to the competitive displacement from negatively charged surfactants present in BALF. However, the release was very low and in all the cases more than 85% of siRNA was retained. TPP cross linked LMWC-29-PS-12 showed higher retention and it was attributed ionic crosslinking. Thus, form the results of the BAL fluid stability study, developed polyplexes were found to be stable in presence of pulmonary fluids.

Table 5.10: % siRNA retained by polyplexes in BALF

Time (min)	% siRNA Retained	
	LMWC-29-PS-12	TPP cross linked LMWC-29-PS-12
0	100.00	100.00
15	98.52±1.44	99.25±1.17
30	97.14±1.91	98.48±2.23
45	96.76±2.33	97.09±2.85
60	94.43±3.08	96.33±1.89
75	92.65±1.72	95.49±3.36
90	92.39±2.14	94.18±2.34
120	88.70±1.68	92.39±3.55

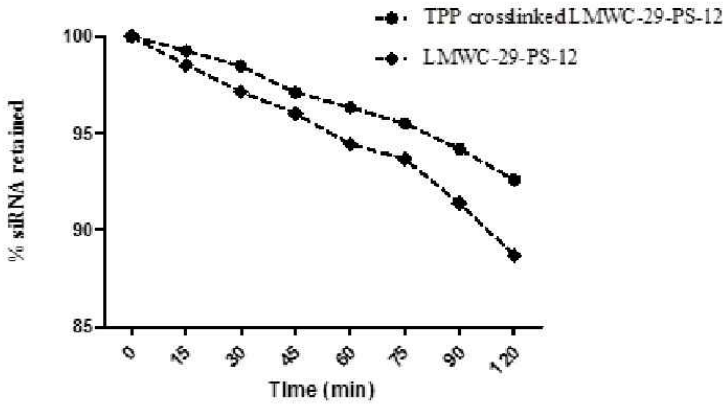

Fig. 5.17: siRNA retained in polyplex at different time points in presence of BAL

5.3.5 Proton Sponge

Fig. 5.18 shows that LMWC-29-PS-12, and TPP crosslinked LMWC-29-PS-12 showed good buffer capacity. Further, TPP crosslinking had no effect on buffer capacity. This was due the presence of LMWC-29 which has pKa in the range of 6.5-6.8, resulting in high buffer capacity in the endosomal pH range [10, 58]. The buffer capacity reported is generally reflection of protonable amine content per unit weight of polymer, which is high in transfection standard, bPEI (1 mole of amine/43 gram moles) compared to chitosan (1 mole amine/179 gram moles) [4]. The bPEI is generally used at polymer to siRNA weight ratio of 0.66 to 1, while chitosan is used at weight ratio of 4 and more. Thus, larger weight ratios of chitosan used can compensate or even exceed amine content in PEI on mole basis and thereby the buffer capacity of bPEI. In addition, literature reports that most of the buffer capacity is derived from the free chitosan part of nucleic-acid complex, due to which chitosan-DNA complex showed ~2 fold reduction in buffering capacity compared to free chitosan, thus engagement of chitosan in nucleic acid binding reduces buffer capacity [10]. In the present case, the binding of siRNA preferentially to PS fraction of conjugate can overcome this effect by providing more unbound chitosan.

On the other hand, PS alone exhibited negligible proton sponge as the titration curve of PS is almost parallel to the solvent curve. This could be due to PS being a peptide rich in arginine amino groups that are all protonated at endosomal pH and consequently

shows poor endosomal escape. This is similar to the scenario of peptides such as poly-L-lysine and poly-L-arginine which have low transfection efficiency.

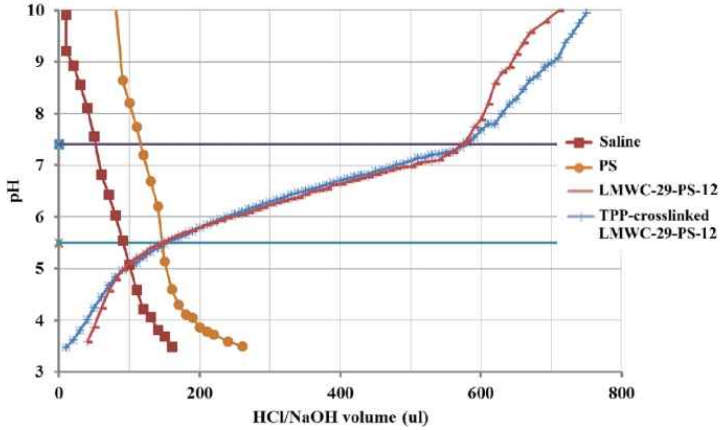

Fig. 5.18: Proton sponge study of chitosan based vectors

5.3.6 Transmission Electron Microscopy

TEM allows direct visible evidence of state of the system rather than indirect measurement such as in DLS. Therefore, TPP cross-linked LMWC-29-PS-12 polyplex i.e. stabilized LMWC-29-PS-12 polyplex were subjected to cryo-TEM evaluation. The TEM images revealed the relatively homogenous internal structure and spherical shape of the particles. TEM showed that the polyplex were discrete and there was no aggregation of polyplex. The TEM image supports the light scattering data.

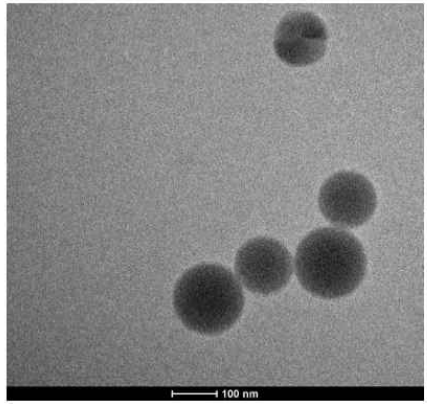

Fig. 5.19: Cryo-TEM image of stabilized LMWC-29-PS-12 polyplex

5.4 References:

1. Shu XZ, Zhu KJ. The influence of multivalent phosphate structure on the properties of ionically cross-linked chitosan films for controlled drug release. European Journal of Pharmaceutics and Biopharmaceutics 2002; 54(2): 235-43.
2. Lee MK, Chun SK, Choi WJ, Kim JK, Choi SH, Kim A, et al. The use of chitosan as a condensing agent to enhance emulsion-mediated gene transfer. Biomaterials 2005; 26(14): 2147-56.
3. Sato T, Ishii T, Okahata Y. In vitro gene delivery mediated by chitosan. effect of pH, serum, and molecular mass of chitosan on the transfection efficiency. Biomaterials 2001; 22(15): 2075-80.
4. Buschmann MD, Merzouki A, Lavertu M, Thibault M, Jean M, Darras V. Chitosans for delivery of nucleic acids. Advanced Drug Delivery Reviews 2013; 65(9): 1234-70.
5. Cifani N, Chronopoulou L, Pompili B, Di Martino A, Bordi F, Sennato S, et al. Improved stability and efficacy of chitosan/pDNA complexes for gene delivery. Biotechnology letters 2015; 37(3): 557-65.
6. Han L, Tang C, Yin C. Effect of binding affinity for siRNA on the in vivo antitumor efficacy of polyplexes. Biomaterials 2013; 34(21): 5317-27.
7. Malmo J. Chitosan-based nanocarriers for gene-and siRNA-delivery. 2012.
8. Ping Y, Liu C, Zhang Z, Liu KL, Chen J, Li J. Chitosan-graft-(PEI-beta-cyclodextrin) copolymers and their supramolecular PEGylation for DNA and siRNA delivery. Biomaterials 2011; 32(32): 8328-41.
9. Dabaghian M, Ebrahimi SM, Nikbakhat Borojeni G, Tebianian M, Rezaei Mokaram A, Iman M, et al. Use of N-trimethyl chitosan for intranasal delivery of DNA encoding M2e-HSP70c in mice. Iranian Journal of Veterinary Medicine 2013; 7(2): 123-28.
10. Richard I, Thibault M, De Crescenzo G, Buschmann MD, Lavertu M. Ionization behavior of chitosan and chitosan–DNA polyplexes indicate that chitosan has a similar capability to induce a proton-sponge effect as PEI. Biomacromolecules 2013; 14(6): 1732-40.

11. Allan GG, Peyron M. Molecular weight manipulation of chitosan. I: Kinetics of depolymerization by nitrous acid. Carbohydr Res 1995; 277(2): 257-72.
12. Lavertu M, Methot S, Tran-Khanh N, Buschmann MD. High efficiency gene transfer using chitosan/DNA nanoparticles with specific combinations of molecular weight and degree of deacetylation. Biomaterials 2006; 27(27): 4815-24.
13. Mao S, Shuai X, Unger F, Simon M, Bi D, Kissel T. The depolymerization of chitosan: effects on physicochemical and biological properties. Int J Pharm 2004; 281(1-2): 45-54.
14. Hermanson GT. Bioconjugate techniques: Academic press; 2013.
15. Chen S. Polymer-coated iron oxide nanoparticles for medical imaging: Massachusetts Institute of Technology; 2010.
16. Saito G, Amidon GL, Lee KD. Enhanced cytosolic delivery of plasmid DNA by a sulfhydryl-activatable listeriolysin O/protamine conjugate utilizing cellular reducing potential. Gene Ther 2003; 10(1): 72-83.
17. Balhorn R, Hud N, Corzett M, Mazrimas J. Importance of protamine phosphorylation to histone displacement in spermatids: can the disruption of this process be used for male contraception. Lawrence Livermore National Lab., CA (United States), 1995.
18. Liu WG, Zhang JR, Cao ZQ, Xu FY, Yao KD. A chitosan-arginine conjugate as a novel anticoagulation biomaterial. J Mater Sci Mater Med 2004; 15(11): 1199-203.
19. Li Z, Ramay HR, Hauch KD, Xiao D, Zhang M. Chitosan–alginate hybrid scaffolds for bone tissue engineering. Biomaterials 2005; 26(18): 3919-28.
20. Tallury P, Kar S, Bamrungsap S, Huang Y-F, Tan W, Santra S. Ultra-small water-dispersible fluorescent chitosan nanoparticles: synthesis, characterization and specific targeting. Chemical Communications 2009; (17): 2347-49.
21. Schreiber SB. Chitosan-gallic acid films as multifunctional food packaging. 2012.
22. Naruphontjirakul P, Viravaidya-Pasuwat K. Development of Doxorubicin–Core Shell O-succinyl Treat Human Cancer. 2011.
23. Zhang J, Li C, Xue Z-Y, Cheng H-W, Huang F-W, Zhuo R-X, et al. Fabrication of lactobionic-loaded chitosan microcapsules as potential drug carriers targeting the liver. Acta biomaterialia 2011; 7(4): 1665-73.

24. Bartczak D, Kanaras AG. Preparation of peptide-functionalized gold nanoparticles using one pot EDC/sulfo-NHS coupling. Langmuir 2011; 27(16): 10119-23.
25. Techaarpornkul S, Wongkupasert S, Opanasopit P, Apirakaramwong A, Nunthanid J, Ruktanonchai U. Chitosan-mediated siRNA delivery in vitro: effect of polymer molecular weight, concentration and salt forms. Aaps Pharmscitech 2010; 11(1): 64-72.
26. Rojanarata T, Opanasopit P, Techaarpornkul S, Ngawhirunpat T, Ruktanonchai U. Chitosan-thiamine pyrophosphate as a novel carrier for siRNA delivery. Pharmaceutical research 2008; 25(12): 2807-14.
27. Lee SJ, Lee A, Hwang SR, Park J-S, Jang J, Huh MS, et al. TNF-[alpha] Gene Silencing Using Polymerized siRNA/Thiolated Glycol Chitosan Nanoparticles for Rheumatoid Arthritis. Mol Ther 2014; 22(2): 397-408.
28. Liu X, Howard KA, Dong M, Andersen MØ, Rahbek UL, Johnsen MG, et al. The influence of polymeric properties on chitosan/siRNA nanoparticle formulation and gene silencing. Biomaterials 2007; 28(6): 1280-88.
29. Ma PL, Buschmann MD, Winnik FM. One-Step Analysis of DNA/Chitosan Complexes by Field-Flow Fractionation Reveals Particle Size and Free Chitosan Content. Biomacromolecules 2010; 11(3): 549-54.
30. Mao S, Shuai X, Unger F, Simon M, Bi D, Kissel T. The depolymerization of chitosan: effects on physicochemical and biological properties. International Journal of Pharmaceutics 2004; 281(1): 45-54.
31. Yang H-C, Hon M-H. The effect of the molecular weight of chitosan nanoparticles and its application on drug delivery. Microchemical Journal 2009; 92(1): 87-91.
32. von Harpe A, Petersen H, Li Y, Kissel T. Characterization of commercially available and synthesized polyethylenimines for gene delivery. J Control Release 2000; 69(2): 309-22.
33. Tallury P, Kar S, Bamrungsap S, Huang YF, Tan W, Santra S. Ultra-small water-dispersible fluorescent chitosan nanoparticles: synthesis, characterization and specific targeting. Chem Commun (Camb) 2009; (17): 2347-9.

34. MacLaughlin FC, Mumper RJ, Wang J, Tagliaferri JM, Gill I, Hinchcliffe M, et al. Chitosan and depolymerized chitosan oligomers as condensing carriers for in vivo plasmid delivery. Journal of Controlled Release 1998; 56(1–3): 259-72.
35. Gamzazade AI, Šlimak VM, Skljar AM, Štykova EV, Pavlova SSA, Rogožin SV. Investigation of the hydrodynamic properties of chitosan solutions. Acta Polymerica 1985; 36(8): 420-24.
36. Holzerny P, Ajdini B, Heusermann W, Bruno K, Schuleit M, Meinel L, et al. Biophysical properties of chitosan/siRNA polyplexes: profiling the polymer/siRNA interactions and bioactivity. J Control Release 2012; 157(2): 297-304.
37. Fan W, Yan W, Xu Z, Ni H. Formation mechanism of monodisperse, low molecular weight chitosan nanoparticles by ionic gelation technique. Colloids Surf B Biointerfaces 2012; 90: 21-7.
38. Pillai CKS, Paul W, Sharma CP. Chitin and chitosan polymers: Chemistry, solubility and fiber formation. Progress in Polymer Science 2009; 34(7): 641-78.
39. Whitehead KA, Langer R, Anderson DG. Knocking down barriers: advances in siRNA delivery. Nat Rev Drug Discov 2009; 8(2): 129-38.
40. Duceppe N, Tabrizian M. Factors influencing the transfection efficiency of ultra low molecular weight chitosan/hyaluronic acid nanoparticles. Biomaterials 2009; 30(13): 2625-31.
41. Liao ZX, Ho YC, Chen HL, Peng SF, Hsiao CW, Sung HW. Enhancement of efficiencies of the cellular uptake and gene silencing of chitosan/siRNA complexes via the inclusion of a negatively charged poly(gamma-glutamic acid). Biomaterials 2010; 31(33): 8780-8.
42. Badawy MEI, Rabea EI. A Biopolymer Chitosan and Its Derivatives as Promising Antimicrobial Agents against Plant Pathogens and Their Applications in Crop Protection. International Journal of Carbohydrate Chemistry 2011; 2011.
43. Cheng W, Tang C, Yin C. Effects of particle size and binding affinity for siRNA on the cellular processing, intestinal permeation, and anti-inflammatory efficacy of polymeric nanoparticles. J Gene Med 2015.
44. Köping-Höggård M. Chitosan Polyplexes as Non-Viral Gene Delivery Systems: Structure-Property Relationships and In Vivo Efficiency. 2003.

45. Liu X, Howard KA, Dong M, Andersen MO, Rahbek UL, Johnsen MG, et al. The influence of polymeric properties on chitosan/siRNA nanoparticle formulation and gene silencing. Biomaterials 2007; 28(6): 1280-8.
46. Peer D, Zhu P, Carman CV, Lieberman J, Shimaoka M. Selective gene silencing in activated leukocytes by targeting siRNAs to the integrin lymphocyte function-associated antigen-1. Proceedings of the National Academy of Sciences 2007; 104(10): 4095-100.
47. Song E, Zhu P, Lee S-K, Chowdhury D, Kussman S, Dykxhoorn DM, et al. Antibody mediated in vivo delivery of small interfering RNAs via cell-surface receptors. Nature biotechnology 2005; 23(6): 709-17.
48. Guo P, Coban O, Snead NM, Trebley J, Hoeprich S, Guo S, et al. Engineering RNA for targeted siRNA delivery and medical application. Advanced Drug Delivery Reviews 2010; 62(6): 650-66.
49. Chono S, Li S-D, Conwell CC, Huang L. An efficient and low immunostimulatory nanoparticle formulation for systemic siRNA delivery to the tumor. Journal of Controlled Release 2008; 131(1): 64-69.
50. Peer D, Park EJ, Morishita Y, Carman CV, Shimaoka M. Systemic leukocyte-directed siRNA delivery revealing cyclin D1 as an anti-inflammatory target. Science 2008; 319(5863): 627-30.
51. REISCHL D, JANTSCHER-KRENN E, BERNHART E, SATTLER W, ZIMMER A. Protamine Based siRNA-Nanoparticles: Particle Composition Dependant Influences on RNA Interference Efficiency. Sci Pharm 2010; 78: 686.
52. Chen J, Yu Z, Chen H, Gao J, Liang W. Transfection efficiency and intracellular fate of polycation liposomes combined with protamine. Biomaterials 2011; 32(5): 1412-18.
53. Rampino A, Borgogna M, Blasi P, Bellich B, Cesàro A. Chitosan nanoparticles: Preparation, size evolution and stability. International Journal of Pharmaceutics 2013; 455(1–2): 219-28.
54. Katas H, Alpar HO. Development and characterisation of chitosan nanoparticles for siRNA delivery. Journal of Controlled Release 2006; 115(2): 216-25.

55. Almalik A, Donno R, Cadman CJ, Cellesi F, Day PJ, Tirelli N. Hyaluronic acid-coated chitosan nanoparticles: molecular weight-dependent effects on morphology and hyaluronic acid presentation. J Control Release 2013; 172(3): 1142-50.
56. Ungphaiboon S, Attia D, Gomez d'Ayala G, Sansongsak P, Cellesi F, Tirelli N. Materials for microencapsulation: what toroidal particles ("doughnuts") can do better than spherical beads. Soft Matter 2010; 6(17): 4070-83.
57. Foster AA, Greco CT, Green MD, Epps TH, 3rd, Sullivan MO. Light-mediated activation of siRNA Release in diblock copolymer assemblies for controlled gene silencing. Adv Healthc Mater 2015; 4(5): 760-70.
58. Dehshahri A, Alhashemi SH, Jamshidzadeh A, Sabahi Z, Samani SM, Sadeghpour H, et al. Comparison of the effectiveness of polyethylenimine, polyamidoamine and chitosan in transferring plasmid encoding interleukin-12 gene into hepatocytes. Macromolecular Research 2013; 21(12): 1322-30.